# The Imine−Pyridine Torsion of the Pyridoxal 5′-Phosphate Schiff Base of Aspartate Aminotransferase Lowers Its p$K_a$ in the Unliganded Enzyme and Is Crucial for the Successive Increase in the p$K_a$ during Catalysis†

Hideyuki Hayashi, Hiroyuki Mizuguchi, and Hiroyuki Kagamiyama*

*Department of Biochemistry, Osaka Medical College, 2-7 Daigakumachi, Takatsuki 569-8686, Japan*

*Received June 25, 1998; Revised Manuscript Received August 24, 1998*

ABSTRACT: In aspartate aminotransferase, pyridoxal 5′-phosphate (PLP) forms a Schiff base with the ϵ-amino group of Lys258 (internal aldimine). The internal aldimine has a p$K_a$ value of 6.8. Binding of a substrate amino acid to the enzyme yields the Michaelis complex, in which PLP still forms the internal aldimine with Lys258. This is followed by a transaldimination process to form a Schiff base of PLP with the α-amino group of substrates (external aldimine). Kinetic analysis of the spectral changes during the reaction of the enzyme with a substrate analogue 2-methylaspartate showed that the aldimine is 6.4−8.6% protonated in the Michaelis complex and 32−43% in the external aldimine. The bases that accept protons from the aldimines are considered to be the substrate α-amino group in the Michaelis complex and the ϵ-amino group of Lys258 in the external aldimine. Therefore, the intrinsic p$K_a$ value of the aldimine is expected to increase over a range of 3 during transformation from the unliganded enzyme (p$K_a$ = 6.8) to the Michaelis complex (p$K_a$ = 8.8) and the external aldimine (p$K_a$ > 10). When the Lys258 side chain of the internal aldimine was "cleaved" by the construction of an enzyme in which Lys258 was replaced by Ala and the aldimine was reconstituted with methylamine, the p$K_a$ of the internal aldimine was increased to 9.6. This indicates that the low p$K_a$ value of the internal aldimine of the unliganded enzyme is provided by the side chain of Lys258 which destabilizes the planar conformation of the aldimine suitable for protonation. This strained conformation is partially relaxed in the Michaelis complex, and the p$K_a$ is moderately increased. On formation of the external aldimine, Lys258 is released and the aldimine is fixed to a near planar conformation and has a high p$K_a$ value. Thus, the aldimine p$K_a$ is modulated by a mechanism that exploits the conformational differences between the intermediate structures. The strain of the protonated internal aldimine is interpreted to enhance the catalytic ability of the enzyme by increasing the energy level of the free enzyme plus substrate at neutral pH relative to the transition state.

From the kinetic studies of aspartate aminotransferase (aspartate: 2-oxoglutarate aminotransferase, EC 2.6.1.1; AspAT)[1] under steady-state (*1*) and transient-state (*2*−*4*) conditions, a mechanism for the reaction of aspartate with AspAT has been proposed (Scheme 1). The PLP−Lys258[2] Schiff base (internal aldimine) of the unliganded enzyme has the imine p$K_a$ value of 6.8, which is strikingly low compared to the value of 12.4 of the PLP−*n*-butylamine Schiff base (*6*). The reaction of aspartate with AspAT begins either by the association of $E_L$ (unprotonated aldimine form) with the triionic form of aspartate ($SH^+$) to generate $E_L{\cdot}SH^+$ or by the association of $E_LH^+$ (protonated aldimine form) with the dianionic form of aspartate (S) to generate $E_LH^+{\cdot}S$ (ref *4*; Scheme 1). The low value of the internal aldimine p$K_a$ increases the fraction of $E_L$, which is the species that accepts $SH^+$, the predominant species at neutral pH (*1*, *4*, *7*). Although the Michaelis complex ($ES_1$) is a mixture of $E_L{\cdot}SH^+$ and $E_LH^+{\cdot}S$, only the latter undergoes transaldimination reaction to yield $ES_2$, in which PLP forms a Schiff base with the substrate amino acid. The PLP−substrate Schiff base is often referred to as an "external aldimine". In $ES_2$, protonation of the aldimine must be favorable for catalysis, because it enhances the electrophilicity of the extended π-electron system and hence will increase the $k_{cat}$ value (*7*, *8*). In accordance with this concept, a recent resonance Raman spectroscopic study (*9*) on the complex of AspAT and 2-methylaspartate (MeAsp), a substrate analogue that stops the catalytic reaction after the formation of $ES_2$, suggested that $ES_2$ is preferentially in the protonated aldimine form ($E_LH^+{=}S$ in Scheme 1). It is of great interest to know the mechanism that lowers the p$K_a$ of the aldimine in the unliganded enzyme and increases the p$K_a$ during the course of the catalysis. The possible protonation of the pyridine N1 of PLP by interaction with Asp222 has been discussed to be

† This work was supported by a research grant from the Japan Society for the Promotion of Science ("Research for the Future" Program 96L00506) and the SUNBOR Grant from Suntory Institute for Bioorganic Research.

* To whom correspondence should be addressed.

[1] Abbreviations: AspAT, aspartate aminotransferase (aspartate: 2-oxoglutarate aminotransferase, EC 2.6.1.1); HEPES, 4-(2-hydroxyethyl)-1-piperadineethanesulfonic acid; MES, 4-morpholineethanesulfonic acid; TAPS, 3−[tris(hydroxymethyl)methyl]aminopropanesulfonic acid; K258A AspAT, AspAT in which the residue Lys258 was replaced by an alanine residue; MeAsp, 2-methylaspartate; K258A-$MeNH_2$ AspAT, K258A AspAT in which the aldimine was reconstituted with methylamine; PLP, pyridoxal 5′-phosphate; PMP, pyridoxamine 5′-phosphate; WT AspAT, wild-type AspAT.

[2] The amino acid residues are numbered according to the sequence of pig cytosolic aspartate aminotransferase (*5*). An asterisk indicates that the residue comes from the neighboring subunit.

10.1021/bi981517e CCC: $15.00 
Published on Web 10/09/1998

Scheme 1: Catalytic Reaction Mechanism of AspAT[a]

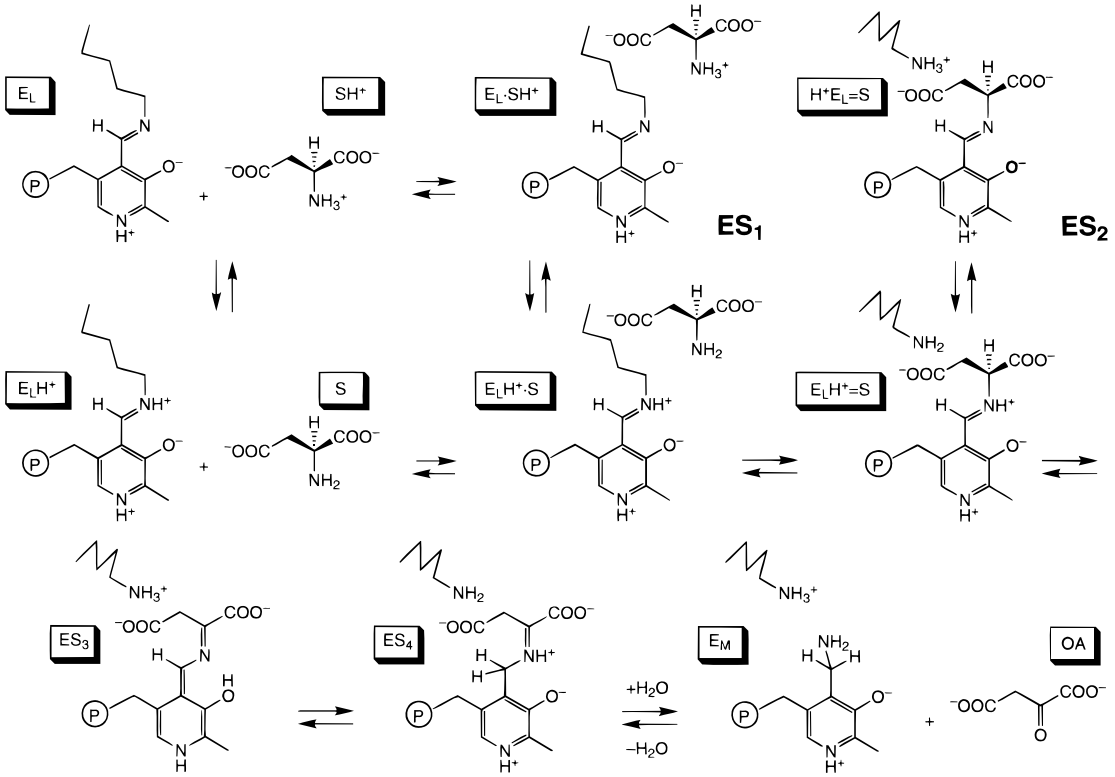


[a] Modified from the scheme in ref *4*. $H^+$ before $E_L$ indicates the protonated Lys258 $\epsilon$-amino group and $H^+$ after $E_L$ indicates the protonated aldimine.

important for lowering the aldimine p$K_a$ in AspAT (*6, 8*). This interaction, however, is not unique to AspAT, and a salt bridge between the pyridine N and an acidic residue of the enzyme is found in the crystallographic structures of D-amino acid aminotransferase (*10*), branched-chain amino acid aminotransferase (*11*), ornithine aminotransferase (*12*), and ornithine decarboxylase (*13*), all of which have high aldimine p$K_a$ values. Thus, protonation of the pyridine N cannot explain the unusually low p$K_a$ value of the AspAT internal aldimine. On the other hand, it has been suggested that the two arginine residues, Arg292* and Arg386 (*14*−*17*), that bind the substrate $\omega$-carboxylate and α-carboxylate groups, respectively, are responsible for the low p$K_a$ value of the internal aldimine of the unliganded enzyme (*7, 8*). Binding of the substrate dicarboxylate neutralizes the positive charges of the two arginine residues and is expected to increase the p$K_a$ values of both the internal aldimine of $ES_1$ and the external aldimine of $ES_2$. Although this hypothesis, first presented by Ivanov and Karpeisky (*7*) and later modified by Kirsch et al. (*8*), gave insight into the fine chemistry of the reaction mechanism of AspAT, there have been several unsolved problems. The absorption spectrum of the AspAT−maleate or AspAT−succinate complex, which mimics $ES_1$, showed that the p$K_a$ of the internal aldimine is 8.2−8.8, compared to 6.3−6.8 of the unliganded enzyme (*18, 19*). On the other hand, the absorption spectrum of the AspAT−MeAsp complex was constant between pH 5.5 and 9.0, showing partial protonation of the aldimine(s) in the complex irrespective of the solution pH (*20*). These different effects of the two kinds of substrate analogues on AspAT cannot be rationalized by the previous electrostatic hypothesis. Furthermore, mutation of these substrate-binding arginine residues to uncharged residues increased the aldimine p$K_a$ by only 0.9−7.7 (*21*). Therefore, neutralization of the positive charges of the arginine residues by substrate carboxylate groups can only partially explain the syncatalytic shifts in the aldimine p$K_a$.

In this study, we first analyzed the spectral transition during the reaction of AspAT with MeAsp and, from the calculated spectra of $ES_1$ and $ES_2$, determined the distribution of the protonated/unprotonated structures of the PLP aldimines in these intermediates and estimated the p$K_a$ transition of the aldimines during the course of the catalysis. Using a mutant enzyme in which Lys258 was replaced by Ala and the aldimine was reconstituted with methylamine, we then showed that the strain on the protonated internal aldimine caused by the Lys258 side chain specifically decreases the p$K_a$ of the internal aldimine without affecting the p$K_a$ of the external aldimine. The modulation of the aldimine p$K_a$ during the course of the catalysis is discussed in a thermodynamic context that the strain of the PLP−Lys258 aldimine increases the free-energy level of the unliganded enzyme at neutral pH and enhances the catalysis.

## EXPERIMENTAL PROCEDURES

*Chemicals. Escherichia coli* AspAT was obtained as previously described (*22*). The PLP form of the K258A AspAT was prepared according to the method of Toney and Kirsch (*23*), except for the use of our pUC19-*aspC* expression system (*22*). The PLP aldimine was reconstituted in K258A AspAT by the addition of 10 mM methylamine. After a 30 min incubation at 298 K, there was no change in the spectrum, with absorption maximum at 421 nm. Further addition of methylamine to 20 mM did not alter the spectrum. DL-2-Methylaspartate (MeAsp) was purchased from Sigma.

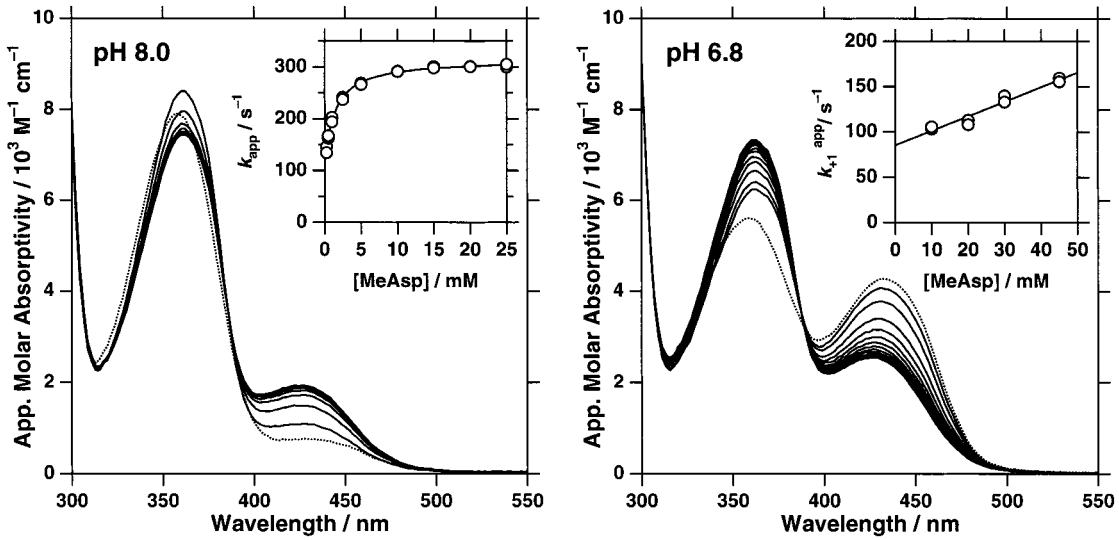


FIGURE 1: (Left) Time-resolved spectra for the reaction of WT AspAT and MeAsp at pH 8.0. Enzyme (40 $\mu$M) and MeAsp (20 mM) were reacted in 50 mM HEPES−NaOH, pH 8.0, containing 0.1 M KCl, at 298 K. Dotted line represents the spectrum of AspAT in the absence of MeAsp. After the addition of MeAsp, the absorption at 430 nm gradually increased with a concomitant decrease in absorption at 360 nm. Spectra were taken between 1.28 and 49.92 ms after mixing with 2.56-ms intervals. Inset shows the plot of the apparent rate constant ($k_{app}$) for the monoexponential absorption change against the concentration of MeAsp. Solid line is the theoretical curve drawn using eq 2. (Right) Time-resolved spectra for the reaction of WT AspAT and MeAsp at pH 6.8. Conditions other than the solution pH were the same as in the left panel. Inset shows the plot of $k_{+1}^{app}$ (eq 4) against the concentration of MeAsp. The $k_{+1}^{app}$ value was obtained from the global analysis of the time-resolved spectra using Glint (see the legend to Figure 2).

The concentrations of MeAsp shown in the text and figures are those of the L isomers.

*Spectroscopic Analysis.* Absorption spectra were measured using a Hitachi U-3300 spectrophotometer at 298 K. The buffer solution contained 50 mM buffer component(s) and 0.1 M KCl. The buffer components used were MES−NaOH, HEPES−NaOH, and TAPS−NaOH. Protein concentrations were generally (1−2) × $10^{-5}$ M in subunit. The concentration of the AspAT subunit in solution was determined spectrophotometrically. The apparent molar extinction coefficients used were $\epsilon_M = 4.7 \times 10^4$ $M^{-1}$ $cm^{-1}$ for the PLP form enzyme and $\epsilon_M = 4.6 \times 10^4$ $M^{-1}$ $cm^{-1}$ for the PMP form enzyme at 280 nm (*3*).

*Kinetic Analysis.* Stopped-flow spectrophotometry was performed using the Applied Photophysics (Leatherhead, UK) SX.17MV system at 298 K. The dead time was generally 2.3 ms under a gas pressure of 500 kPa. The exponential absorption changes were analyzed with the program provided with the instrument. Time-resolved spectra were collected using the SX.17MV system equipped with a photodiode array accessory and the XScan (ver. 1.0) control software. The global analysis of the data was performed using the Marquardt−Levenberg algorithm on Glint (ver. 3.20, Applied Photophysics).

## RESULTS AND DISCUSSION

*Kinetic Analysis of the Reaction of AspAT with 2-Methylaspartate and Resolution of the Spectra of the Michaelis Complex and the External Aldimine.* The reaction of AspAT with 2-methylaspartate (MeAsp) was studied at pH 8.0 (Figure 1 left). At this pH, AspAT exhibits a predominant absorption band at 358 nm with a small one at 430 nm. On association with MeAsp, a rapid and small increase in the intensity of the 360 nm absorption band with a shift of $\lambda_{max}$ to 362 nm occurred during the dead time. This was followed by a gradual decrease in absorption at 362 nm with a concomitant increase in absorption at 430 nm (Figure 1, left; see refs *20* and *22*). This spectral change was found to proceed monoexponentially, and the apparent rate constants ($k_{app}$) for the change were obtained at various MeAsp concentrations. The plot of $k_{app}$ against [MeAsp] (Figure 1, left, inset) showed that the results are most simply interpreted by assuming a two-step mechanism.

$$E^\circ + S^\circ \underset{}{\overset{K_d^{app}}{\rightleftharpoons}} ES_1 \underset{k_{-2}^{app}}{\overset{k_{+2}^{app}}{\rightleftharpoons}} ES_2 \qquad (1)$$

where E° and S° denote the unliganded enzyme ($E_L$ plus $E_LH^+$ in Scheme 1) and the free ligand (MeAsp), respectively. As the reaction of MeAsp with AspAT has been known to stop at $ES_2$ in Scheme 1, the two intermediates in eq 1 are reasonably assigned to $ES_1$ and $ES_2$. The first step is considered to be sufficiently faster than the second, because $k_{app}$ would show a linear dependency on [MeAsp] if the first step is slower than the second. According to eq 1, $k_{app}$ is expressed as

$$k_{app} = \frac{[S]}{K_d^{app} + [S]} k_{+2}^{app} + k_{-2}^{app} \qquad (2)$$

Fitting the experimental data to eq 2 yields the values for the parameters: $K_d^{app} = 1.4 \pm 0.1$ mM, $k_{+2}^{app} = 200 \pm 4$ $s^{-1}$, and $k_{-2}^{app} = 110 \pm 4$ $s^{-1}$. In the presence of 20 mM MeAsp, where almost complete association of AspAT with MeAsp is expected, the spectrum at $t = 0$, obtained by extrapolation of the time-resolved spectra, is considered to represent that of $ES_1$. The absorption spectrum of AspAT after the spectral change is completed (Figure 1, left, $t = 49.92$ ms) is a mixture of the spectra of $ES_1$ and $ES_2$. Therefore, using the values for $k_{+2}^{app}$ and $k_{-2}^{app}$, we could calculate the spectra of the $ES_1$ and $ES_2$ (Figure 2, left). The spectra indicated that

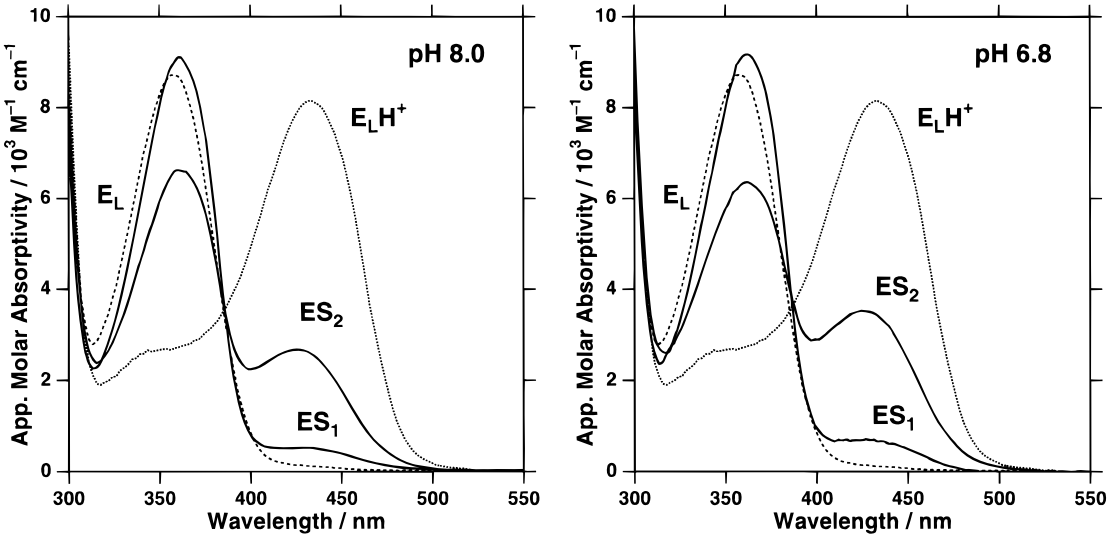


FIGURE 2: Calculated absorption spectra of $ES_1$ and $ES_2$ of the complex of AspAT with MeAsp at pH 8.0 (left) and at pH 6.8 (right). The spectra of $E_L$ (dashed lines) and $E_LH^+$ (dotted lines) are taken from ref *24* and are shown for comparison. The spectra of the intermediates were obtained from the Glint global analysis of the time-resolved spectra of Figure 1. For the data taken at pH 8.0, a reaction scheme "A<>B", corresponding to $ES_1 \rightleftarrows ES_2$ of eq 2, was entered into the model entry box, and the parameters of "k + 1" and "k − 1", corresponding to $k_{+2}^{app}$ and $k_{-2}^{app}$ of eq 2, were fixed to 200 $s^{-1}$ and 110 $s^{-1}$, respectively. For the data taken at pH 6.8, a reaction scheme "A>B, B<>C", corresponding to eq 4, was entered. The initial values for the parameters k + 1, k + 2, and k − 2, corresponding to $k_{+1}^{app}$, $k_{+2}^{app}$, and $k_{-2}^{app}$ of eq 4, were 90, 200, and 110 $s^{-1}$, respectively. The spectrum of A ($E_LH^+$) was fixed by loading the spectrum of $E_LH^+$ (*24*) whose wavelength resolution had been adjusted to that used here. The amount of E° in eq 1 and $E_L$ in eq 3 can be negligible due to the high concentration of MeAsp (over 10 mM). In each global analysis, according to the manufacturer's instruction, a theoretical data set was generated by numerical integration, and the sum of the squares of the residuals was minimized using the Marquardt−Levenberg algorithm. The optimized spectra of A and B generated from the data set at pH 8.0, and those of B and C generated from the data set at pH 6.8, represent the spectra of $ES_1$ and $ES_2$, respectively.

the aldimine is almost unprotonated in $ES_1$, and partially protonated in $ES_2$ at pH 8.0.

To examine whether the spectra of these intermediates change with pH, we performed a similar experiment at pH 6.8, where $E_L$ and $E_LH^+$ exist in equal amounts. On reaction with MeAsp, the absorption at 430 nm decreased with a concomitant increase in absorption at 360 nm (Figure 1, right), and the final spectrum matched closely that obtained at pH 8.0 (Figure 1, left). The time-resolved spectra at pH 6.8 showed a gradual transition from the initial to the final spectra, and the spectrum of $ES_1$, which transiently emerged during the reaction at pH 8.0, was not obviously observed. This is because the spectral change through the successive formation of $ES_1$ and $ES_2$ is masked by the slow interconversion of $E_L$ and $E_LH^+$ at pH 6.8 (*4*). Assuming that the association of MeAsp with AspAT proceeds in the same way as that of aspartate with AspAT (*4*), we can write the following scheme for the reaction of MeAsp with AspAT:

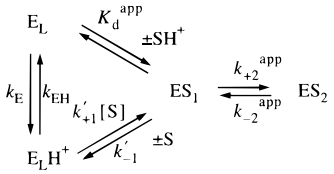


This model assumes a rapid association of the triionic form of MeAsp ($SH^+$) with $E_L$. If there is sufficient concentration of MeAsp, $[E_L]$ would rapidly decrease to zero, and eq 3 can be simplified as follows:

$$E_LH^+ \xrightarrow{k_{+1}^{app}} ES_1 \underset{k_{-2}^{app}}{\overset{k_{+2}^{app}}{\rightleftharpoons}} ES_2 \qquad (4)$$

where $k_{+1}^{app} = k_{EH} + k'_{+1}[S]$. The initial concentrations of the species at pH 6.8 (equal to the aldimine p$K_a$ of the unliganded enzyme) are considered to be as follows: $[E_LH^+] = [ES_1] = [E_t]/2$ and $[ES_2] = 0$, where $[E_t]$ is the total concentration of the enzyme. The spectrum of $E_LH^+$ is already known (*24*). Under these constraints, the time-resolved spectra in Figure 1 (right) were fitted to the model of eq 4 (Glint, ver. 3.20, Applied Photophysics). With 20 mM MeAsp, the rate constants were obtained to be $k_{+1}^{app} = 100 \pm 30$ $s^{-1}$, $k_{+2}^{app} = 210 \pm 60$ $s^{-1}$, and $k_{-2}^{app} = 120 \pm 50$ $s^{-1}$. The values of the latter two parameters were essentially identical to those obtained at pH 8.0. The obtained spectra are shown in Figure 2 (right), and the dependency of $k_{+1}^{app}$ on [MeAsp] is shown in the inset of Figure 1 (right). Extrapolation of $k_{+1}^{app}$ to [MeAsp] = 0 yields $k_{EH} = 85$ $s^{-1}$. As the p$K_a$ value for the α-amino group of MeAsp[3] is 10.6, [S] is equal to $10^{-10.6}/(10^{-10.6} + 10^{-6.8})$ [MeAsp]. Therefore, we could calculate the values of $k'_{+1}$ to be $1.0 \times 10^7$ $M^{-1}$ $s^{-1}$. The value of $k_{EH}$ is in good agreement with the value previously determined from the pH-jump method (*4*), and the value of $k'_{+1}$ is of the same order as that of aspartate ($5.4 \times 10^6$ $M^{-1}$ $s^{-1}$; ref *4*), supporting the validity of the models of eqs 3 and 4 for the analysis of the reaction of MeAsp with AspAT at low pH. The spectra of $ES_1$ and $ES_2$ at pH 6.8 showed striking resemblance to those at pH 8.0 (Figure 2). Using the molar absorptivity of 8700 $M^{-1}$ $cm^{-1}$ at 430 nm for $E_LH^+$ (*24*), we estimated the fraction of the protonated form of the aldimine in $ES_1$ and that in $ES_2$ to be 6.4 and 32%, respectively, at pH 8.0, and 8.6 and 43%, respectively, at

[3] Higaki, T. and Tanase, S. (Kumamoto University), personal communication.

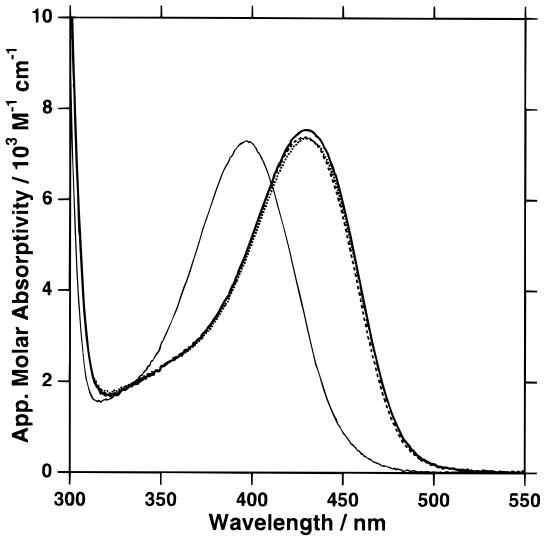


FIGURE 3: Spectra of K258A AspAT complexed with MeAsp. Absorption spectra of K258A AspAT were taken in the presence of 5 mM MeAsp, 50 mM buffer component, and 0.1 M KCl at 298 K. Solid line: pH 8.0 (50 mM HEPES−NaOH). Dotted line: pH 5.7 (50 mM MES−NaOH). Dashed line: pH 9.6 (50 mM TAPS−NaOH). The spectrum of K258A AspAT without MeAsp at pH 8.0 (50 mM HEPES−NaOH) is shown in a thin solid line ($\lambda_{max}$ = 395 nm).

pH 6.8. Thus, both in $ES_1$ and $ES_2$ the aldimines are partially protonated at the imine N. That the spectra of $ES_1$ and $ES_2$ and the rate constants connecting them do not vary with pH explains the pH-independent spectrum of the AspAT−MeAsp complex (ref *20*; Figure 1).

*Proton Shuttling in ES*$_1$ and $ES_2$. The pH-independent spectra of $ES_1$ and $ES_2$ indicate that in each complex the proton shuttles between the aldimine and another base inside the enzyme. In $ES_1$, which is the mixture of $E_L{\cdot}SH^+$ and $E_LH^+{\cdot}S$ (Scheme 1), the base is apparently the α-amino group of MeAsp. In $ES_2$, the ϵ-amino group of Lys258 is the candidate for the base (*20*). This was tested by preparing the external aldimine of PLP with MeAsp in K258A AspAT. Due to the absence of the ϵ-amino group of Lys258 that competes with MeAsp for the formation of the aldimine with PLP, the K258A AspAT−MeAsp complex is considered to be exclusively in the $ES_2$ form. The absorption spectrum showed that the aldimine is almost completely protonated (Figure 3). This indicates that in $ES_2$ the ϵ-amino group of Lys258 is the base that accepts the proton, giving rise to the equilibrium mixture of $E_LH^+{=}S$ and $H^+E_L{=}S$ (Scheme 1). The untitratable nature of the aldimines in $ES_1$ and $ES_2$ is probably due to the instability of $E_LH^+{\cdot}SH^+$ ($H^+E_LH^+{=}S$) and $E_L{\cdot}S$ ($E_L{=}S$). In the $E_LH^+{\cdot}SH^+$ ($H^+E_LH^+{=}S$) structure, the two positive charges on the aldimine and the amino group would cause electrostatic repulsion, while in the $E_L{\cdot}S$ ($E_L{=}S$) structure the lone-pair electrons on the amino group would interact unfavorably with those of the aldimine N and/or the negative charge of the phenolic O3′ of PLP.

The 6.4−8.6% protonation of the internal aldimine in $ES_1$ is in accordance with the results obtained from the Raman spectroscopic study (*9*), which showed that the population of the protonated form of the aldimine in $ES_1$ is less than 10%. However, the Raman study suggested that the aldimine in $ES_2$ is largely protonated and that the equilibrium is shifted from $ES_2$ toward $ES_1$ by a factor of ∼5 (*9*). This may be ascribed to underestimation of the unprotonated form of the aldimine in $ES_2$, which is probably due to measuring the height of the peak in the noisy area of the Raman signals (*9*).

*Sequential Increase in the Intrinsic p$K_a$ of the Aldimine during Catalysis.* The population (6.4−8.6%) of the $E_LH^+{\cdot}S$ structure in $ES_1$ indicates that the intrinsic[4] p$K_a$ of the internal aldimine of $ES_1$ is 1.0−1.2 units lower than that of the α-amino group of MeAsp in the active site. In the unliganded state, the internal aldimine has a p$K_a$ value of 6.8, and on the binding of maleate, a desamino analogue of aspartate, the p$K_a$ increases to 8.8 in the *E. coli* AspAT (*19*). This is considered to be equal to the intrinsic p$K_a$ of the internal aldimine of $ES_1$. Therefore, the intrinsic p$K_a$ of the α-amino group of MeAsp in $ES_1$ is estimated to be 9.8−10.0, which is slightly lower than the value (10.6) in aqueous solutions.[3] It has been argued that the binding of aspartate to the active site of AspAT is accompanied by neutralization of the negative charges of the α- and β-carboxylate groups of aspartate by the positive charges of Arg386 and Arg292*, respectively, and decreases the p$K_a$ of the α-amino group from 9.6 to 7.4 (*8*), which was estimated from the p$K_a$ value of aspartic acid dimethyl ester (*25*). The present results indicate that the p$K_a$ of the α-amino group of MeAsp decreases only 0.6−0.8 on its binding to AspAT. It should be noted that a salt bridge between a carboxylate group and a guanidinium group forms a dipole and does not lead to complete neutralization of the negative charge of the carboxylate. Therefore, we consider that the 2.2 unit decrease in the p$K_a$ of the α-amino group of aspartate, previously reported (*8*), is an overestimation.

The population of the $E_LH^+{=}S$ structure in $ES_2$ (32−43%) indicates that the intrinsic p$K_a$ of the aldimine is 0.1−0.3 unit lower than that of the ϵ-amino group of Lys258. The spectrum of K258A AspAT complexed with MeAsp at pH 9.4 is almost similar to that at pH 5.7 (Figure 3), showing the intrinsic p$K_a$ value of its aldimine to be greater than 10. Accordingly, the intrinsic p$K_a$ value of the ϵ-amino group of Lys258 in $ES_2$ should be similar to (or higher than) the value of lysine in aqueous solutions, 10.5. In the apoenzyme, however, the ϵ-amino group of Lys258 has been reported to have a p$K_a$ value of 8.0 (*26*). In $ES_2$, the presence of the phosphate group of PLP and dicarboxylic amino acid substrates (analogues) in the active site may increase the p$K_a$ of the ϵ-amino group of Lys258 through electrostatic interaction.

The above discussions demonstrated that the (intrinsic) p$K_a$ of the PLP aldimine increases from 6.8 of the free enzyme to 8.8 in $ES_1$, and over 10 in $ES_2$. As described in the introductory portion of this paper, no mechanism presented hitherto can fully explain these p$K_a$ values, that is, the low p$K_a$ in the unliganded enzyme and the successive increase in the p$K_a$ during the course of catalysis. To solve this problem, we first investigated the factors that decrease the p$K_a$ of the PLP−Lys258 aldimine.

[4] For a set of electrostatically coupled dissociation groups, the microscopic p$K_a$ of any one of the groups is affected by the dissociation state of the other groups. The term "intrinsic p$K_a$" used here is the p$K_a$ in the absence of other groups of interest. For a case in which a proton shuttles between dissociation groups A and B, the equilibrium between $AH^+{\cdot}B$ (proton resides on A) and $A{\cdot}H^+B$ (proton resides on B) is independent of pH, and the equilibrium constant, $K_{eq} = [AH^+{\cdot}B]/[A{\cdot}BH^+]$, is approximately equal to $10^{(pK_a^A - pK_a^B)}$, where $pK_a^A$ and $pK_a^B$ are the "intrinsic" p$K_a$ values of A and B, respectively.

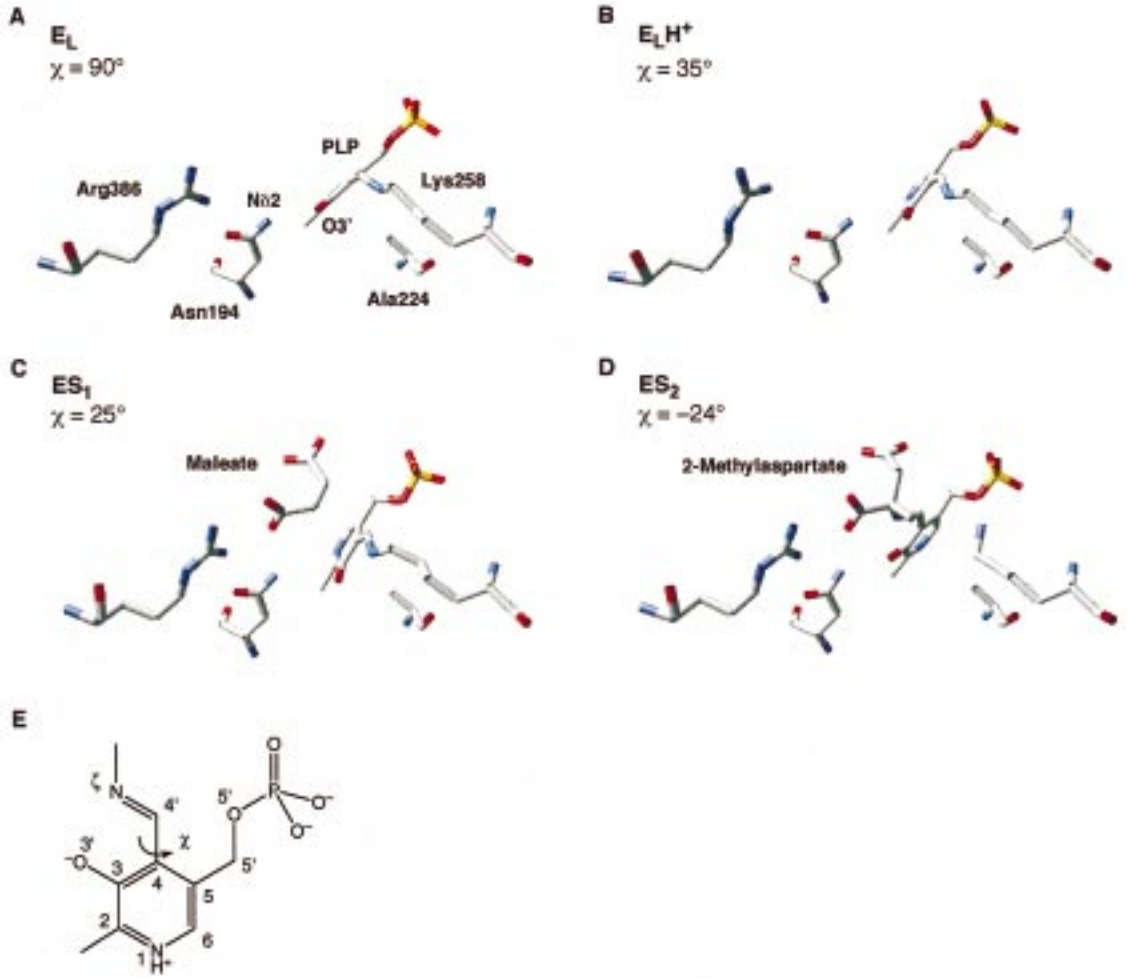


FIGURE 4: Active-site structures of AspAT. (A) Unliganded enzyme at pH 7.0 (ref *17*; PDB entry code 1ARS, 1.8 Å resolution). (B) Unliganded enzyme at pH 5.4 (ref *15*; 1AJR, 1.74 Å). The $\chi$ value is the average of those of the two subunits. (C) Maleate-bound form at pH 7.0 (1ASM, 2.35 Å). The $\chi$ value is the average of those of 1ASM and 1ASA (2.4 Å). (D) MeAsp-bound form at pH 7.0 (ref *17*; 1ART, 1.8 Å). A, C, and D: *E. coli* enzyme. B: pig cytosolic enzyme. C and D are considered to be models for $ES_1$ and $ES_2$, respectively. (E) Numbering of the atoms of the PLP aldimine and definition of $\chi$. For D, N is that of the α-amino group of MeAsp.

*Strain on the PLP−Lys258 Aldimine.* The crystal structures of AspATs from chicken mitochondria (*16*) and *E. coli* (*17*) at high pH (7.5 and 7.0, respectively) showed that the imine bond of the aldimine is almost perpendicular to the plane of the pyridine ring (Figure 4A). Crystallographic analysis on the *E. coli* AspAT at low pH has not yet been carried out. Recently, however, Arnone and colleagues (*15*) published high-resolution crystallographic data on the pig cytosolic enzyme at pH 5.4, where most of the aldimine is protonated. The *E. coli* AspAT at pH 7.0 and the pig cytosolic AspAT at pH 5.4 are both in open forms, and the active-site structures except for PLP and Lys258 are superimposable. Therefore, we considered that the structure of the pig cytosolic enzyme at pH 5.4 can be used as a model for the aldimine-protonated structure of *E. coli* AspAT.[5] The structure showed that the protonated imine bond (C4′−N$\delta$) is close to the plane of the pyridine ring (Figure 4B). As the imine bond is tethered to the protein backbone via the Lys258 side chain, only a 36−44° rotation of the imine bond around C4−C4′ is allowed, and a compensatory rotation of the pyridine ring around the N1−C4 axis is required to generate a planar structure of the PLP−Lys258 aldimine. However, the rotation of the pyridine ring cannot go further than 14−16° due to the van der Waals contact of the pyridine ring with the methyl group of Ala224 (Figure 4, panels A and B). Additionally, the hydrogen bond between O3′ of PLP and N$\delta$2 of Asn194 seems to restrict the rotation of the pyridine ring (Figure 4, panels A, B). As a result, the torsion angle of C3−C4−C4′−N$\zeta$, expressed as $\chi$ (Figure 4E), cannot be smaller than 30−40°, and the PLP−Lys258 aldimine bears a significant strain at this position (Figure 4B). To determine the effect of this strain on the p$K_a$ value of the aldimine, we constructed an enzyme in which the side chain of Lys258 was cleaved at the aliphatic portion and studied its spectrophotometric properties. The enzyme was prepared by reconstituting the PLP aldimine in K258A

[5] The study by McPhalen et al. (*16*) is a direct comparison of the $E_L$ (pH 7.5; PDB 7AAT) and $E_LH^+$ (pH 5.1; PDB 8AAT) structures of the same enzyme (chicken mitochondrial AspAT) at 1.9 and 2.3 Å resolutions, respectively. The $E_LH^+$ structure shows that the C4−C4′ bond is out of the plane of the pyridine ring to the *si* face by 18°, and because of this deviation the $\chi$ angle is close to 0°. The 18° deviation can be considered to provide a strain energy similar to that discussed in this paper. However, the C4−C5−C5′−O5′ torsion angle ($\phi$) of the $E_L$ structure of this enzyme is −45°, compared to −16° of that of *E. coli* AspAT (Figure 4A). As the transition from the $E_L$ to the $E_LH^+$ structure is expected to increase the $\phi$ value, we consider the $E_LH^+$ structure of the pig cytosolic enzyme ($\phi$ = 38°, Figure 4B) to be a better model for the $E_LH^+$ structure of *E. coli* AspAT than that of the chicken mitochondrial enzyme ($\phi$ = −16°).

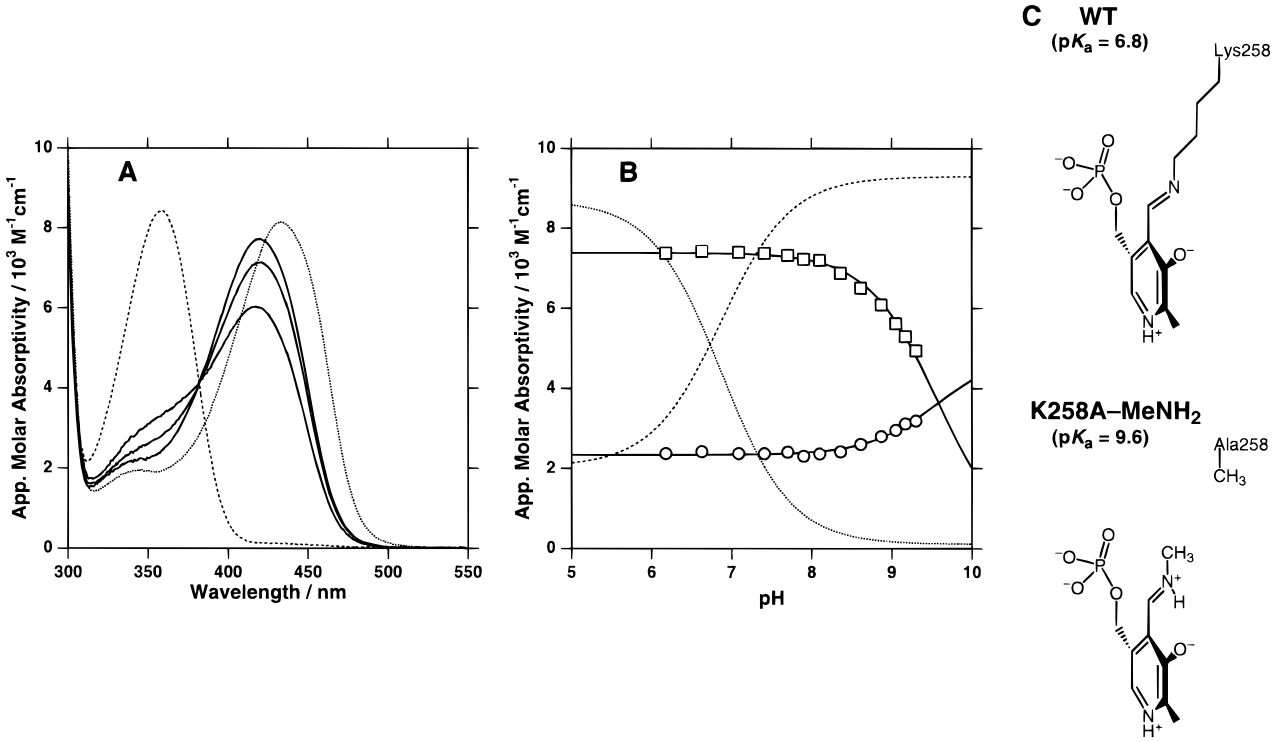


FIGURE 5: (A) Absorption spectra of K258A-MeNH$_2$ AspAT. From top to bottom of the 421-nm absorption peak, pH 8.0, 8.8, and 9.4. Dotted and dashed lines are the spectra of $E_LH^+$ ($\lambda_{max}$ = 430 nm) and $E_L$ ($\lambda_{max}$ = 358 nm) of WT AspAT, respectively. (B) Plot of the apparent molar absorption coefficients at 360 nm (circles) and at 421 nm (squares). The theoretical lines are drawn using the equation $\epsilon_{app} = [10^{-pK_a}/(10^{-pK_a} + 10^{-pH})]\epsilon_E + [10^{-pH}/(10^{-pK_a} + 10^{-pH})]\epsilon_{EH}$, where $\epsilon_E$ and $\epsilon_{EH}$ represent the molar absorption coefficients of $E_L$ and $E_LH^+$, respectively. Fitting the theoretical lines to the experimental values gave the p$K_a$ value of 9.6. For comparison, the pH dependency of the apparent absorption coefficients of WT AspAT (p$K_a$ = 6.8) at 360 nm (dashed line) and at 430 nm (dotted line) are shown. (C) Schematic drawings of the PLP aldimines and the residue 258 side chains of WT and K258A-MeNH$_2$ AspATs.

AspAT with methylamine (Figure 5C; hereafter we refer to the aldimine-reconstituted enzyme as K258A-MeNH$_2$ AspAT).

*PLP Aldimine of K258A-MeNH$_2$ AspAT Has a High p$K_a$ Value and a Relaxed Conformation.* K258A AspAT has an absorption maximum at 395 nm (*23*), which is derived from the free aldehyde form of PLP. On addition of 10 mM methylamine at pH 8.0, it showed an absorption maximum at 421 nm (Figure 5A). The spectrum resembles that of the $E_LH^+$ form of the wild-type (WT) AspAT, although the absorption maximum is blue-shifted (430 nm for WT AspAT). This indicates that methylamine forms an aldimine with PLP in K258A-MeNH$_2$ AspAT, and the aldimine is protonated at pH 8.0, where most of the aldimine of WT AspAT is unprotonated. With increasing pH, the absorbance of K258A-MeNH$_2$ AspAT at 421 nm gradually decreased with a concomitant increase in absorbance at 350−360 nm, showing deprotonation of the PLP−methylamine aldimine (Figure 5A). The p$K_a$ of the aldimine was determined to be 9.6 by plotting the absorbance values at 421 and 358 nm against the pH (Figure 5B).

The CD spectra of the $E_L$ and $E_LH^+$ forms of WT AspAT show strong positive CD bands at 358 and 430 nm, respectively, corresponding to the absorption maxima of the two forms (*6*, *24*, *27*). These CD bands are considered to arise partly from the torsion of the PLP−Lys258 aldimine at the C4−C4′ bond,[6] since distorted $\pi$-electron systems have been known to show CD maxima corresponding to the $\pi-\pi^*$ transition (*28*). The CD spectra of K258A-MeNH$_2$ AspAT showed little Cotton effect over 300 nm compared to the $E_LH^+$ form of WT AspAT (Figure 6). It is reasonable to consider that this reflects the planar conformation of the aldimine of K258A-MeNH$_2$ AspAT. Combining all the previous results, we can now assume that the linkage of PLP to the enzyme protein via the Lys258 side chain causes the strain on the protonated form of the PLP−Lys258 aldimine and decreases its p$K_a$ from 9.6 to 6.8.

*Thermodynamic Interpretation of the PLP−Lys258 Aldimine p$K_a$.* To understand quantitatively the mechanism by which the strain decreases the p$K_a$ of the aldimine, we made a thermodynamic interpretation of the relationship between the p$K_a$ and the conformation of PLP aldimines. The proton dissociation of a PLP aldimine is expressed thermodynamically:

$$\mu^\circ_{AldH^+}(\chi) + RT\ln[AldH^+] = \mu^\circ_{Ald}(\chi) + RT\ln[Ald] + \mu^\circ_{H^+} + RT\ln[H^+] \quad (5)$$

where $\mu^\circ_{AldH^+}(\chi)$, $\mu^\circ_{Ald}(\chi)$, and $\mu^\circ_{H^+}$ denote the standard chemical potentials of the protonated aldimine, deprotonated aldimine, and proton, respectively. The dependence of

[6] Another interpretation of the CD band is that PLP is bound in an asymmetric environment (*29*). According to this, the reduced CD of K258A-MeNH$_2$ AspAT may reflect loss of the asymmetric binding mode of PLP, and may not directly indicate the decreased torsion angle of the aldimine. However, the maleate-bound WT AspAT (see text) and the D222A AspAT (see PDB 1ASA and 1ASB), both of which have relaxed conformations of the PLP aldimine, have reduced molar CD/molar absorptivity ($\Delta\epsilon/\epsilon$) values at 430 nm [$2.3 \times 10^{-3}$ for the maleate-bound WT AspAT (unpublished data) and $1.7 \times 10^{-3}$ for D222A AspAT (*30*)] compared to that of the unliganded WT AspAT [$3.0 \times 10^{-3}$ (*24*)]. We consider that this supports, at least partially in AspAT, the hypothesis correlating the CD signal with the torsion angle of the aldimine.

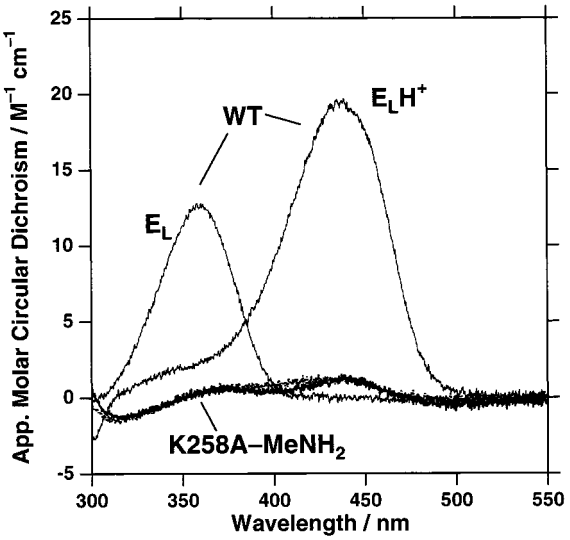


FIGURE 6: Circular dichroism spectra of WT and K258A-MeNH$_2$ AspATs. Spectra of K258A-MeNH$_2$ AspAT were taken at pH 8.0 (solid line, 50 mM HEPES−NaOH) and pH 9.4 (dotted line, 50 mM TAPS−NaOH), containing 0.1 M KCl. These two spectra are almost superimposable. Molar circular dichroism values of WT AspAT in the $E_L$ form ($\Delta\epsilon_E$) and in the $E_LH^+$ form ($\Delta\epsilon_{EH}$) were calculated from the values at pH 5.6 (50 mM MES−NaOH, 0.1 M KCl) and pH 8.0 (50 mM HEPES−NaOH, 0.1 M KCl), using the equation $\Delta\epsilon_{app} = [10^{-pK_a}/(10^{-pK_a} + 10^{-pH})]\Delta\epsilon_E + [10^{-pH}/(10^{-pK_a} + 10^{-pH})]\Delta\epsilon_{EH}$.

$\mu^\circ_{AldH^+}(\chi)$ and $\mu^\circ_{Ald}(\chi)$ on $\chi$ was estimated by the calculation of the heat of formation of the two structures of the pyridoxal−methylamine aldimine at each $\chi$. It was shown that $\mu^\circ_{AldH^+}(\chi)$ increases and $\mu^\circ_{Ald}(\chi)$ decreases monotonically with increasing $|\chi|$ (see the shapes of the curves in Figure 7). Therefore, the protonated aldimine takes the conformation where $|\chi|$ has the minimum value and the unprotonated aldimine takes the conformation where $|\chi|$ has the maximum value. It can be interpreted that the planar conformation of the protonated aldimine is stabilized by the internal hydrogen bond between the imine N and O3′, whereas, in the deprotonated aldimine, the nonplanar conformation is taken to avoid the electrostatic repulsion of the lone pair electrons of the imine N and those of O3′. The repulsion energy seems to be greater than the resonance stabilization energy of the pyridine-imine $\pi$-conjugation.

When the solution pH is equal to the p$K_a$ of the aldimine, that is, $[AldH^+] = [Ald]$, eq 5 is transformed to:

$$\mu^\circ_{AldH^+}(|\chi|_{min}) = \mu^\circ_{Ald}(|\chi|_{max}) + \mu^\circ_{H^+} + RT\ln(10^{-pK_a}) \quad (6)$$

This describes the relationship between the conformational constraint, defined by $|\chi|_{min}$ and $|\chi|_{max}$, and the p$K_a$ of the aldimine. For K258A-MeNH$_2$ AspAT, as $0° \le \chi \le 90°$, we obtain

$$\mu^\circ_{AldH^+}(0°) = \mu^\circ_{Ald}(90°) + \mu^\circ_{H^+} + RT\ln(10^{-9.6}) \quad (7)$$

Equation 7 determines the relative positions of the potential curves of $\mu^\circ_{AldH^+}(|\chi|)$, which is dependent on $|\chi|$, and $\mu^\circ_{Ald}(|\chi|) + \mu^\circ_{H^+} + RT\ln[H^+]$, which is dependent on both $|\chi|$ and the pH (Figure 7). In WT AspAT and its reaction-intermediate complexes, the range of the values allowed for $\chi$ is determined by the interactions of the aldimines with the surrounding residues. For a given set of $|\chi|_{min}$ and $|\chi|_{max}$, the p$K_a$ of the aldimine can be determined from eq 6 and Figure 7. In the unliganded WT AspAT, the $\chi$ value is restricted to a range $(35 \pm 5)° \le \chi \le 90°$ (Figure 4, panels A and B). Figure 7 shows that $\mu^\circ_{AldH^+}(35°)$ is equal to $\mu^\circ_{Ald}(90°) + \mu^\circ_{H^+} + RT\ln(10^{-6.8})$ and explains the p$K_a$ value of 6.8 for the aldimine of the unliganded WT AspAT.

The mechanism presented here can explain the unusually high aldimine p$K_a$ values found in several mutant AspATs. Protonation at the PLP pyridine N1 stabilized by the negative charge of Asp222 has the unequivocal effect of lowering the p$K_a$ of the imine of PLP aldimines by 2.5, which is calculated from studies on model compounds in aqueous solutions (*6*). The [Asp222 → Ala] AspAT, however, showed an extremely high p$K_a$ value, which cannot be obtained by pH titration up to 10 (*30*) and exceeds the estimated p$K_a$ value ($6.8 + 2.5 = 9.3$). Because Asp222 is an important residue to which PLP anchors its pyridinium ring, mutation on the residue would unwind the torsion of the PLP−Lys258 aldimine and may further increase its p$K_a$. Mutation of Asn194 to Ala increases the PLP−Lys258 aldimine by 1.3 (*19*). It has been unclear why a replacement without altering the charge of the side chain (Asn to Ala) caused a significant increase in the p$K_a$ value. It can now be considered that the removal of the hydrogen bond from Asn194 N$\delta$2 to PLP O3′ relaxed partially the strain of the aldimine. Combining the present and the earlier studies altogether, we propose that the p$K_a$ value of the PLP−Lys258 aldimine is decreased by 2.8 through the strain of the Lys258 side chain, 2.5 through the protonation at pyridine N, and 0.9 through the electrostatic interactions with the two arginine residues. The sum of these values, 6.2, can roughly explain the decrease in p$K_a$ from 12.4 of the PLP−*n*-butylamine aldimine (corresponding to the side chain of Lys258) to 6.8 of AspAT, although the discrepancy of 0.6 suggests that the p$K_a$ of the aldimine is somewhat increased by incorporating the aldimine into the active site of the enzyme.

*Mechanism of Modulation of the Aldimine p$K_a$ in the Catalytic Intermediates.* The values of the aldimine p$K_a$ in the intermediate complexes, $ES_1$ and $ES_2$, can be interpreted in the same way as above. In the maleate-bound AspAT, which is considered to mimic the $ES_1$ structure, the N$\delta$2 of Asn194 forms a new hydrogen bond (length = 3.1 Å) with the maleate carboxylate and weakens the hydrogen bond to O3′ of PLP (the N$\delta$2-O3′ distance increases from 2.8 to 3.3 Å; comparison of the structures 1ASN and 1ASM deposited in PDB). This will partially relax the strain of the protonated PLP−Lys258 aldimine (Figure 4, panels B and C), and $\chi$ can be as low as 20−30°. This low $|\chi|_{min}$ value increases the aldimine p$K_a$ to around 8.1 (Figure 7). In addition, the neutralization of the positive charges of Arg292* and Arg386 by the two carboxylate groups of the substrate will further increase the p$K_a$ by 0.9 to 9.0 (*21*), which roughly coincides with the p$K_a$ of the AspAT−maleate complex (the model for $ES_1$). In accordance with this conjecture, the p$K_a$ of the PLP−Lys258 aldimine of N194A mutant AspAT increased by only 1, corresponding to the "pure" electrostatic effect, on the binding of maleate (*19*).

In $ES_2$, the Lys258 side chain is released from the coenzyme. The PLP−aspartate aldimine is fixed to the enzyme protein mainly via its two carboxylate groups and the phosphate group (Figure 4D). As a consequence, the imine bond does not move so freely as that of the PLP−

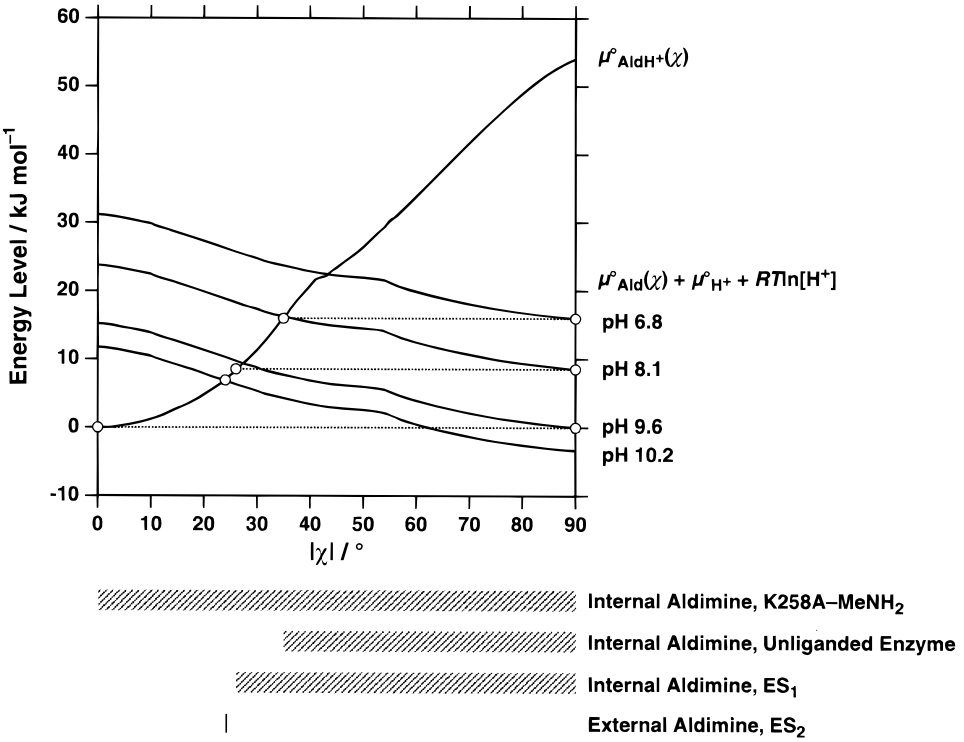


FIGURE 7: Standard chemical potentials for the protonated form [$\mu^\circ_{AldH^+}(\chi)$] and the unprotonated form [$\mu^\circ_{AldH}(\chi)$] of PLP aldimine as functions of $\chi$. The structure of the pyridoxal−methylamine aldimine either protonated or unprotonated at the imine N (but always protonated at N1 and unprotonated at O3′) was geometrically optimized at every $\chi$ value with 1° intervals, and the value of the heat of formation for each conformer was used to draw the potential curves. The program used for optimization is MOPAC6 bundled to Cerius[2] (ver. 3.5, Molecular Simulations, Inc.) with PM3 Hamiltonian. The proton chemical potential ($\mu^\circ_{H^+} + RT\ln[H^+]$) was added to $\mu^\circ_{Ald}(\chi)$ for direct comparison of the chemical potentials of the two forms. The bottom horizontal bars show the region allowed for $|\chi|$ of the respective aldimine structures. The value of $\mu^\circ_{AldH^+}(0)$ ($=\mu^\circ_{Ald}(90°) + \mu^\circ_{H^+} + RT\ln(10^{-9.6})$) was taken as zero. The curves for $\mu^\circ_{Ald}(\chi) + \mu^\circ_{H^+} + RT\ln[H^+]$ are the same in shape but have different positions depending on pH.

Lys258 aldimine, and the value of $\chi$ is considered to be fixed at −24° (*15*). Thus, the curves of $\mu^\circ_{AldH^+}(\chi°)$ and $\mu^\circ_{Ald}(\chi°) + \mu^\circ_{H^+} + RT\ln(H^+)$ should intersect at $\chi = -24°$, and the p$K_a$ of the aldimine is estimated to be 10.2 (Figure 7). This explains the high aldimine p$K_a$ (>10) of this intermediate.

A decrease in the aldimine p$K_a$ of the unliganded enzyme is caused by destabilization of $E_LH^+$ relative to $E_L$. However, factors that destabilize $E_LH^+$, such as electrostatic effects on PLP, tend to cause destabilization of $E_LH^+$═S, resulting in the accumulation of the dead-end intermediate $H^+E_L$═S. The decrease in the aldimine p$K_a$ through the imine−pyridine torsion, described in this paper, is the mechanism that can destabilize $E_LH^+$ without affecting the energy level of $E_LH^+$═S.

*Aldimine p$K_a$ Value of ES$_1$.* In $ES_1$, the equilibrium between $E_L$·$SH^+$ and $E_LH^+$·S is shifted toward $E_L$·$SH^+$ by a factor of 10−15. As $E_LH^+$·S is the species obligatory for transaldimination (to yield $H^+E_L$═S), this equilibrium shift seems to be unfavorable for catalysis. However, in the actual catalysis, the substrate is aspartate, which has the α-amino group p$K_a$ 1.0 unit lower than that of MeAsp. Therefore, the fraction of $E_LH^+$·S in $ES_1$ formed between AspAT and aspartate is considered to be 43−48%. The rate constant for the transaldimination from $E_LH^+$·S to $E_LH^+$═S is estimated to be 2300−3100 $s^{-1}$, using the $k_{+2}^{app}$ value (200 $s^{-1}$) and the fraction (6.4−8.6%) of the protonated aldimine of $ES_1$ for the reaction of AspAT with MeAsp. Therefore, the apparent rate constant ($k_{+2}^{app}$) for the net transaldimination from $ES_1$ to $ES_2$ of the actual catalysis is calculated to be 1000−1500 $s^{-1}$. This is sufficiently greater than the $k_{cat}$ value of 550 $s^{-1}$ for the half reaction of AspAT with aspartate (*3*). The 2 unit increase in the p$K_a$ of the aldimine on the formation of the Michaelis complex is therefore considered to be the marginal value required for the transaldimination reaction not to be rate limiting in the entire catalytic process.

*Use of Enzyme Strain Energy for Catalysis.* Several methods have been considered to be used by enzymes to optimize their catalytic ability; acid−base catalysis, covalent catalysis, metal catalysis, approximation, transition-state binding, and strain (*31*). Among them, "strain" of the substrate in the Michaelis complex caused by the enzyme−substrate association force has been discussed to increase the $k_{cat}$ value of the enzyme (*31*). However, it does not increase the $k_{cat}/K_m$ value because it reduces the affinity of the substrate (*32*). The present study discussed the strain

[7] The free energy levels expressed by the closed panels relative to that of the transition state in Figure 8 are not experimentally obtained ones. Due to the uncertainty of the position of the methylamine released after the transaldimination of the PLP−methylamine aldimine with a substrate amino acid, the free-energy level of the transition state for the catalytic reaction of K258A-$MeNH_2$ AspAT cannot be compared with that of WT AspAT. In this respect, the technology developed by Gloss and Kirsch (*33*) that introduces various lysine analogues (homo-Lys's) to position 258 by alkylating K258C AspAT is of interest, because it can alter the strain on the PLP−homo-Lys258 aldimine through changing the flexibility of the side chain of homo-Lys. However, the presence of a sulfur atom inside the side chain significantly decreases the p$K_a$ of the ω-amino group, and the effects of changing the strain on the aldimine p$K_a$ value and the energy level of the transition state are difficult to evaluate. Incorporation of non-sulfur homo-Lys's to position 258 through in vitro expression may provide a solution to this problem.

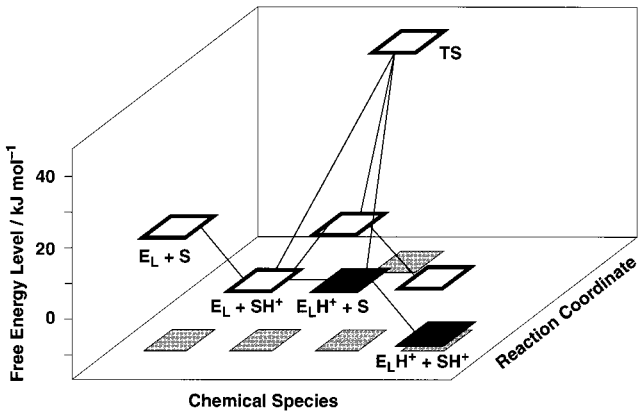


FIGURE 8: Diagram showing the free-energy levels of the free enzyme ($E_L$, $E_LH^+$) plus substrate (S, $SH^+$) and the transition state (TS) of the reaction of AspAT with aspartate at pH 7.0. The energy level of $E_L + SH^+$ was taken as zero. The energy levels of $E_L$ + S, $E_LH^+$ + S, and $E_LH^+ + SH^+$ were calculated using the p$K_a$ values of the α-amino group of aspartate and the PLP−Lys258 aldimine, 9.6 and 6.8, respectively. The energy level of the transition state is calculated from the $k_{cat}^{half}/K_m^{half}$ value for aspartate at pH 8.0 ($1.2 \times 10^6$ $M^{-1}$ $s^{-1}$; ref *3*) and the Eyring equation (*32*). If the strain on the protonated structure of the PLP−Lys258 aldimine is released and the aldimine p$K_a$ is increased to 9.6, the energy levels of $E_LH^+$ + S and $E_LH^+ + SH^+$ will be those represented by closed panels. Hatched squares at the bottom represent the shadows of the panels indicating the chemical species and the reaction coordinates.

energy of the unliganded enzyme, not the substrate. Figure 8 illustrates how the enzyme strain energy is used to increase the $k_{cat}/K_m$ value of AspAT. If there is no strain on the PLP−Lys258 aldimine, the free energy levels of $E_LH^+$ + S and $E_LH^+ + SH^+$ would be such as expressed by the closed panels,[7] and $E_LH^+ + SH^+$ has the lowest free-energy level. In AspAT, the strain on the protonated PLP aldimine raises the free energy level of $E_LH^+$. The energy level of the starting state (the unliganded enzyme plus the free substrate) is therefore increased and the free-energy gap between the transition and the starting states is decreased. Through this explanation, it is apparent why AspAT has chosen a mechanism that destabilizes $E_LH^+$ rather than stabilizes $E_L$ to decrease the p$K_a$ of the PLP−Lys258 aldimine.

The present study showed that the strain of the PLP aldimine caused by the Lys258 side chain lowers the p$K_a$ of the internal aldimine without lowering the intrinsic p$K_a$ of the external aldimine. This is an elaborated mechanism that confers on AspAT both high $k_{cat}/K_m$ and $k_{cat}$ values. The "enzyme strain energy" is a new concept that may be listed among the factors that are used by enzymes for the optimization of catalytic ability. Therefore, it is of great interest whether there are additional examples that share a similar mechanism of utilizing "enzyme strain" for catalysis with AspAT, in the enzymes carrying cofactors and, more generally, enzymes without cofactors.

## REFERENCES


1. Kiick, D. M., and Cook, P. F. (1983) *Biochemistry 22*, 375−382.
2. Fasella, P., and Hammes, G. G. (1967) *Biochemistry 6*, 1798−1804.
3. Kuramitsu, S., Hiromi, K., Hayashi, H., Morino, Y., and Kagamiyama, H. (1990) *Biochemistry 29*, 5469−5476.
4. Hayashi, H., and Kagamiyama, H. (1997) *Biochemistry 36*, 13558−13569.
5. Ovchinnikov, Yu., Egorov, C. A., Aldanova, N. A., Feigina, M. Yu., Lipkin, V. M., Abdulaev, N. G., Grishin, E. V., Kiselev, A. P., Modyanov, N. N., Braunstein, A. E., Polyanovsky, O. L., and Nosikov, V. V. (1973) *FEBS Lett. 29*, 31−34.
6. Kallen, R. G., Korpela, T., Martell, A. E., Matsushima, Y., Metzler, C. M., Metzler, D. E., Morozov, Yu. V., Ralston, I. M., Savin, F. A., Torchinsky, Yu. M., and Ueno, H. (1985) in *Transaminases* (Christen, P., and Metzler, D. E., Eds.) pp 37−108, John Wiley & Sons, New York.
7. Ivanov, V. I., and Karpeisky, M. Y. (1969) *Adv. Enzymol. Relat. Areas Mol. Biol. 32*, 21−53.
8. Kirsch, J. F., Eichele, G., Ford, G. C., Vincent, M. G., Jansonius, J. N., Gehring, H., and Christen, P. (1984) *J. Mol. Biol. 174*, 497−525.
9. Deng, H., Goldberg, J. M., Kirsch, J. F., and Callender, R. (1993) *J. Am. Chem. Soc. 115*, 8869−8870.
10. Sugio, S., Petsko, G. A., Manning, J. M., Soda, K., and Ringe, D. (1995) *Biochemistry 34*, 9661−9669.
11. Okada, K., Hirotsu, K., Sato, M., Hayashi, H., and Kagamiyama, H. (1997) *J. Biochem. 121*, 637−641.
12. Shen, B. W., Hennig, M., Hohenester, E., Jansonius, J. N., and Schirmer, T. (1998) *J. Mol. Biol. 277*, 81−102.
13. Momany, C., Ernst, S., Ghosh, R., Chang, N. L., and Hackert, M. L. (1995) *J. Mol. Biol. 252*, 643−655.
14. Arnone, A., Rogers, P. H., Hyde, C. C., Briley, P. D., Metzler, C. M., and Metzler, D. E. (1985) in *Transaminases* (Christen, P., and Metzler, D. E., Eds.) pp 138−154, John Wiley & Sons, New York.
15. Rhee, S., Silva, M. M., Hyde, C. C., Rogers, P. H., Metzler, C. M., Metzler, D. E., and Arnone, A. (1997) *J. Biol. Chem. 272*, 17293−17302.
16. McPhalen, C. A., Vincent, M. G., and Jansonius, J. N. (1992) *J. Mol. Biol. 225*, 495−517.
17. Okamoto, A., Higuchi, T., Hirotsu, K., Kuramitsu, S., and Kagamiyama, H. (1994) *J. Biochem. 116*, 95−107.
18. Jenkins, W. T., and D'Ari, L. (1966) *J. Biol. Chem. 241*, 5667−5674.
19. Yano, T., Mizuno, T., and Kagamiyama, H. (1993) *Biochemistry 32*, 1810−1815.
20. Fasella, P., Giartosio, A., and Hammes, G. G. (1966) *Biochemistry 5*, 197−202.
21. Kagamiyama, H., Hayashi, H., Yano, T., Mizuguchi, H., and Ishii, S. (1994) in *Biochemistry of Vitamin B6 and PQQ* (Marino, G., Sannia, G., and Bossa, F., Eds.) pp 43−47, Birkhäuser, Basel, Switzerland.
22. Inoue, Y., Kuramitsu, S., Inoue, K., Kagamiyama, H., Hiromi, K., Tanase, S., and Morino, Y. (1989) *J. Biol. Chem. 264*, 9673−9681.
23. Toney, M. D., and Kirsch, J. F. (1993) *Biochemistry 32*, 1471−1479.
24. Hayashi, H., Inoue, K., Nagata, T., Kuramitsu, S., and Kagamiyama, H. (1993) *Biochemistry 32*, 12229−12239.
25. Perrin, C. (1965) *Dissociation Constants of Organic Bases in Aqueous Solution*, pp 353−404, Butterworths, London, U.K.
26. Slebe, J. C., and Martinez-Carrion, M. (1976) *J. Biol. Chem. 251*, 5663−5669.
27. Sterk, M., and Gehring, H. (1991) *Eur. J. Biochem. 201*, 703−707.
28. Kochendoerfer, G. G., Verdegem, P. J. E., van der Hoef, I., Lugtenburg, J., Richard A., and Mathies, R. A. (1996) *Biochemistry 35*, 16230−16240.
29. Ben-Kasus, T., Markel, A., Gdalevsky, G. Ya., Torchinsky, Yu. M., Phillips, R. S., and Parola, A. H. (1996) *Biochim Biophys Acta 1294*, 147−152.
30. Yano, T., Kuramitsu, S., Tanase, S., Morino, Y., and Kagamiyama, H. (1992) *Biochemistry 31*, 5878−5887.
31. Jencks, W. P. (1969) *Catalysis in Chemistry and Enzymology*, McGraw-Hill, New York.
32. Fersht, A. L. (1985) *Enzyme Structure and Mechanism*, pp 331−334, Freeman, New York.
33. Gloss, L. M., and Kirsch, J. F. (1995) *Biochemistry 34*, 3990−3998.


BI981517E